

## RESEARCH ARTICLE

# A link adaptation scheme for the downlink of mobile hotspot

Md. M. Hasan, Jon W. Mark and X. Shen\*

Department of Electrical and Computer Engineering, University of Waterloo, Waterloo, ON N2L 3G1, Canada

## ABSTRACT

A link adaptation (LA) scheme for the downlink of mobile hotspot, which is supported by an IEEE 802.16e or mobile WiMAX network, is proposed. The mobile WiMAX uses orthogonal frequency division multiple access (OFDMA) in its physical layer. The main function of the LA scheme is to select an appropriate burst profile, which includes a multiple input multiple output (MIMO) transmission mode, modulation technique, and coding scheme. We formulate a discrete optimization problem for the LA scheme by maximizing the throughput. An algorithm to implement the LA scheme is also proposed. Numerical results show that the proposed LA scheme exhibits good performance. Copyright © 2011 John Wiley & Sons, Ltd.

## KEYWORDS

link adaptation; mobile hotspot; WiMAX; MIMO; OFDMA

### \*Correspondence

X. Shen, Department of Electrical and Computer Engineering, University of Waterloo, Waterloo, ON N2L 3G1, Canada.

E-mail: xshen@bcr.uwaterloo.ca

## 1. INTRODUCTION

The term mobile hotspot refers to a hotspot, e.g., a wireless local area network (WLAN), located in a moving platform such as a vehicle. It provides Internet access to its terminals. There is no unified system architecture for supporting mobile hotspots over wireless networks [1–4]. In this paper, we adopt the wireless wide area network (WWAN)–WLAN-based system architecture described in [4–6]. In this system architecture, there are two network segments: upward and downward. The upward network segment is a WWAN and the downward network segment is a WLAN within a high velocity vehicle. The vehicle can be a bus or train. Larger area coverage is required to reduce handoff rate. We choose mobile WiMAX for WWAN because of its extended mobility support and larger area coverage [7]. Moreover, the physical dimensions of WiMAX base station (BS) and mobile hotspot are suitable for a multiple input multiple output (MIMO)-based antenna system, which is capable of providing larger antenna element separation. The system architecture is shown in Figure 1.

The WiMAX BS is an entity of cellular WiMAX network. The BS is connected to Internet through a wireline or an optical fiber link. The access point (AP) is mounted within the mobile hotspot. The AP communicates with the BS through the roof top antenna system. It acts as a

mobile router or gateway for the downward network, i.e., the WLAN within the mobile hotspot. The AP is just an interface between two types of networks. It has two separate antenna systems to communicate with each type of network segment. All the mobile nodes (MNs) within the vehicle are connected with the AP through the IEEE 802.11n based WLAN. These MNs can be laptops or other handheld devices, which are carried by the passengers. In this paper, our focus is restricted to the WiMAX-based network segment. More specifically, we are interested in the downlink portion between the WiMAX BS and the AP of mobile hotspot.

The link adaptation (LA) scheme selects a burst profile based on channel state information. As the mobile hotspots move with high velocity, the channel state changes rapidly. The burst profiles must be adaptive with the channel state to gain expected level of performance. In the literature, there are some proposed LA techniques for mobile WiMAX [8–10]. We mention three such techniques because they deal with similar problems as ours. A static threshold table based LA is proposed in [8], which is the simplest technique. The table is prepared based on a pedestrian channel model and a target forward error correcting (FEC) block error rate (FBER), and indicates the threshold signal-to-noise ratios (SNRs) for the different burst profiles. This LA technique requires only the SNR information to select an appropriate burst profile, while important issues, such as higher

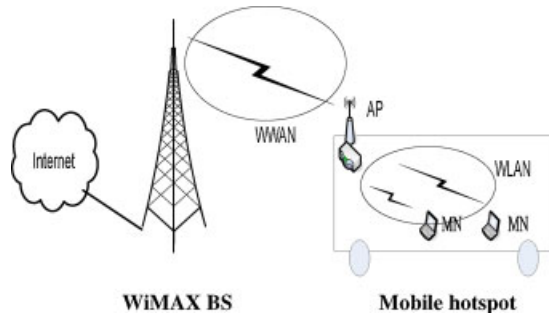


Figure 1. System architecture for mobile hotspot.

mobility, MIMO channel correlations, error tracking, etc., are ignored. A Moore's finite state based LA technique is proposed in [9]. Each burst profile represents a state. Basically, two separate LA techniques are proposed: a channel state technique and an error technique. In the channel state technique, an attenuation factor is used to select the burst profile. This approach is theoretical rather than practical. In the error technique, a number of successive erroneous frames is used to select the burst profile. It selects a lower order modulation if a certain number of failures occur, and selects a higher order modulation if a certain number of successful deliveries occur. The MIMO features and channel coding are ignored in both techniques. Moreover, the system becomes complicated as the number of states increases. A dynamic threshold LA (DTLA) algorithm is proposed in [10]. It dynamically sets and updates the SNR thresholds for different burst profiles. It selects an appropriate burst profile based on the SNR threshold and a Demmel condition number [11]. No error tracking mechanism, such as automatic-repeat-request (ARQ), is considered in DTLA. The DTLA algorithm is not high mobility specific and consists of many feedback loops. It also ignores the sub-channelization and the power allocation issues.

Our proposed LA algorithm uses a static threshold table of SNR per symbol, with the SNR dynamically adjusted before performing table lookup. This adjustment is done based on mobility state. Our algorithm also considers MIMO channel correlation and an adaptive ARQ mechanism for error tracking. The major contributions in this paper are four-fold: (1) proposal of an LA algorithm; which is dedicated to high velocity vehicles; (2) incorporation of a medium access control (MAC) layer error control mechanism into our LA algorithm; (3) introduction of a velocity-based SNR adjustment; and (4) introduction of a MIMO mode switching parameter. The proposed LA algorithm requires only two types of information: information on channel response and ACK/NACK message status of each frame. As per IEEE 802.16e standard, it is mandatory for the mobile WiMAX BS to record and update these information on a frame-by-frame basis. Therefore, there is no additional load on the network.

The remainder of the paper is organized as follows. The system model is described in Section 2. The problem under consideration is formulated in Section 3. The proposed LA

scheme is presented in Section 4. Numerical results are presented in Section 5, and concluding remarks are given in Section 6.

## 2. SYSTEM MODEL

We consider a single cell, single user (only one mobile hotspot) scenario. The BS is located at the center of the cell. An omni-directional antenna system is mounted on top of the BS. Unlike the traditional mobile systems, such as GSM and CDMA, the BS of mobile WiMAX is capable of processing complicated tasks. The entire mobile hotspot itself is the mobile station (MS). The APs are much more powerful compared to an ordinary MS within the WLAN. Moreover, the physical dimensions of the APs are suitable for the MIMO-based antenna systems, which can improve data rate and reliability. A MIMO system can be operated either in a space-time block code (STBC) mode or in a spatial multiplexing (SM) mode. The STBC mode improves transmission reliability by using diversity. On the other hand, the SM mode improves transmission data rate by using multiplexing. In our system, we consider a  $2 \times 2$  MIMO system which can switch between these two modes based on channel condition. This type of MIMO system was first proposed in [12]. Any vehicle has a velometer to measure its velocity; our mobile hotspot is also equipped with a velometer to measure its velocity accurately. This is another good feature of the mobile hotspots, whereas the ordinary MS or MN could not measure its velocity. This information has a very important use in our SNR estimation.

We model the downlink scenario between the BS and an AP of a mobile hotspot as shown in Figure 2. The mobile WiMAX uses a combination of MIMO and orthogonal frequency division multiple access (OFDMA); we will use the term MIMO-OFDMA to describe our system. A MIMO-OFDMA transmitter is located at the BS and a MIMO-OFDMA receiver is located at the AP. The signals are transmitted through a multipath fading channel, assumed to exhibit flat Rayleigh fading with additive white Gaussian noise (AWGN). There exists an  $N_t \times N_r$  MIMO

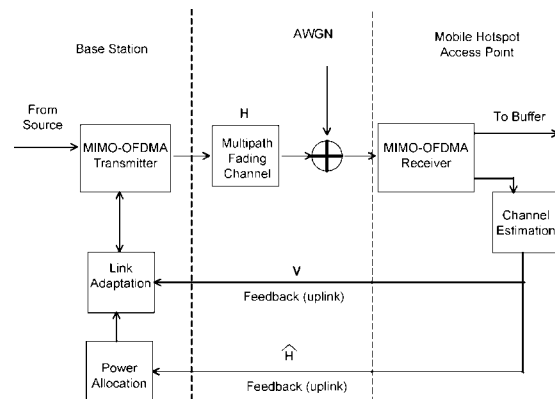


Figure 2. Downlink system model.

antenna array between the transmitter and the receiver, where  $N_t$  and  $N_r$  are the numbers of antenna elements at the transmitter and the receiver, respectively. At the receiver, the information bits are extracted from the data subchannels<sup>†</sup> and fed to the buffer. The pilot subcarriers are fed to the channel estimation block. This block estimates the channel responses for each subcarrier and records the current velocity of the vehicle (mobile hotspot) from the velometer. The channel estimator then sends this information to the BS by using the uplink subframe. A power allocation block works at the BS to allocate power among the subcarriers. The power allocator also computes the estimated post-detection SNR for each subcarrier. The LA block selects the appropriate burst profiles for each subchannel. It gets the SNR values from the power allocation block and collects information on the ARQ blocks of the previous downlink subframe and current velocity. If an ARQ block in the previous downlink subframe is not acknowledged by the subsequent uplink subframe or negatively acknowledged (NACK), then retransmissions are performed up to a certain limit. ARQ is a part of the MAC layer, although this is not explicitly shown on the figure. Our main interest is in the LA block, where our algorithm will work. The transmitter gets the information on burst profile from the LA block.

### 3. PROBLEM FORMULATION

We use the term ‘burst profile’ to describe the combination of modulation and coding, and MIMO transmission. Note that inter-subchannel power allocation is not considered as part of the LA; we leave it as a component of resource allocation (RA). However, we will discuss intra-subchannel power allocation in the next section. Our LA algorithm uses some necessary information: effective SNR per subchannel at the receiver end, FBER requirement, and ACK/NACK messages of ARQ blocks of the previous downlink subframe. Our criterion for the derivation of the LA algorithm is throughput maximization. The burst profile with higher spectral efficiency is deployed to achieve higher throughput. The corresponding burst profile must meet the system bit error rate (BER) requirement. We set this BER to correspond to a prescribed FBER. Ultimately, BER and FBER are both functions of SNR. The BS gets the channel response information from the AP. Most LA techniques define an SNR threshold level for each burst profile and compare the current SNR with the SNR threshold to make a decision about the switching of burst profile. Unfortunately, exact SNR information is not available due to imperfection in estimation techniques and time varying nature of the wireless channel. Therefore, error tracking is required to make a proper selection of burst profile. We use NACK messages of the previous downlink subframe ARQ blocks as the warning signals in our LA algorithm. These signals

are useful to select burst profile for the next downlink subframe. Another important factor is the velocity; it is evident that the velocity of vehicles (mobile hotspot in our case) has a significant impact on system throughput and packet error rate. We consider the impact of velocity in our SNR estimation procedures in the next section. Our LA problem can be formulated as a discrete optimization problem. We solve the same problem separately for each subchannel. This is due to the fact that different subchannel has different effective SNR. Roughly, the effective SNR of a subchannel is the geometric mean of its member subcarriers’ SNR. We formulate our LA problem to ensure efficient spectrum usage with a satisfactory level of FBER. The dimension of one FEC block is one subchannel by two OFDMA symbol duration. A burst profile for each subchannel is selected for each downlink subframe. The generalized form of our optimization problem is as follows:

$$\text{maximize } R_{i,k}(x) \quad (1)$$

$$\text{subject to } q_{i,k}(x) \leq Q \quad \forall i \quad (2)$$

$$\text{and } p_i(\eta_i, \rho) > 0 \quad \forall i \quad (3)$$

$$i \in \{1, 2, 3, \dots, U\}$$

where  $R_{i,k}(x)$  is the throughput for burst profile  $i$ , subchannel  $k$ , and effective SNR  $x$ .  $i$  is the burst profile index, and  $U$  is the number of possible burst profiles in our system.  $q_{i,k}(x)$  is the FBER for burst profile  $i$ , subchannel  $k$ , and effective SNR  $x$ .  $Q$  is the maximum tolerable FBER.  $p_i(\eta_i, \rho)$  is the priority function for burst profile  $i$ . We set three pre-conditions for subchannel  $k$ : (1) it is allocated to the mobile hotspot; (2) some power is allocated to subchannel  $k$ ; and (3) subchannel  $k$  does not carry information for more than one ARQ block for the same mobile hotspot (in the same downlink subframe). We also assume that the allocated power is sufficient to meet the SNR requirement of at least one burst profile. The priority function, a function of the spectral efficiency  $\eta_i$  and erroneous reception indicator  $\rho$ , is an additional constraint introduced to adapt the erroneous reception of the corresponding ARQ block in the previous downlink (DL) subframe. It is a measure of the performance of the previous DL subframe transmission. Higher values of this function indicate higher priorities and *vice versa*. It takes zero in case of inappropriate burst profiles. We define the priority function as:

$$p_i(\eta_i, \rho) = \eta_i I_{\{q_{i,k}(x) \leq Q\}} \left[ I_{\{i = \underset{j}{\operatorname{argmax}} \eta_j I_{\{q_{j,k}(x) \leq Q\}}\}} I_{\{\rho=0\}} + I_{\{i \neq \underset{j}{\operatorname{argmax}} \eta_j I_{\{q_{j,k}(x) \leq Q\}}\}} I_{\{\rho \geq 0\}} \right] \quad (4)$$

$$\text{for } \sum_i^U I_{\{q_{i,k}(x) \leq Q\}} \geq 2$$

<sup>†</sup> In OFDMA PHY of WiMAX, a subchannel is the minimum allocation unit in the frequency domain. It consists of a number of subcarriers [13].

$$= \eta_i I_{\{q_{i,k}(x) \leq Q\}} \text{ for } \sum_i^U I_{\{q_{i,k}(x) \leq Q\}} = 1 \quad (5)$$

where  $\eta_i$  is the spectral efficiency of burst profile  $i$ ;  $I_{\{\cdot\}}$  is the indicator function which takes the value 1 or 0 depending on satisfaction of condition;  $\rho$  takes the value 0 if the corresponding ARQ block in the previous downlink subframe was successfully received and 1 for erroneous reception;  $i, j \in \{1, 2, 3, \dots, U\}$  are the indices for the burst profiles.

The main reason behind introducing this function is that: if the corresponding ARQ block in the previous DL subframe is erroneously received, we may select the burst profile with the second highest spectral efficiency instead of the highest spectral efficiency. It will ensure more reliable transmission at the cost of spectral efficiency.

If the size of a FEC block is  $L_b$  bits and  $P_b$  is the BER, then the upper bound of FBER is given by:

$$q \leq 1 - (1 - P_b)^{L_b} \quad (6)$$

Equation (6) is true with equality when all bits are equally likely to be in error [14].

The spectral efficiency of a burst profile with an M-ary modulation scheme, coding rate  $r$ , and spatial code rate  $\mu$  is given by

$$\eta = \mu r \log_2 M \quad (7)$$

The normalized throughput for M-ary modulation with code rate  $r$  and spectral efficiency  $\eta$  can be written as

$$R = (1 - q)\eta \text{ bps/Hz} \quad (8)$$

## 4. PROPOSED LA SCHEME

As our proposed LA algorithm is static threshold based, we construct the SNR threshold tables. These tables will indicate the minimum SNRs required corresponding to the burst profiles. The SNR thresholds are selected based on modulation order, coding scheme, and MIMO transmission mode. Higher order modulation demands higher SNR threshold and *vice versa*. We consider QPSK  $\frac{1}{2}$ , QPSK  $\frac{3}{4}$ , 16-QAM  $\frac{1}{2}$ , 16-QAM  $\frac{3}{4}$ , 64-QAM  $\frac{2}{3}$ , and 64-QAM  $\frac{3}{4}$  for the STBC mode, and 16-QAM  $\frac{1}{2}$ , 16-QAM  $\frac{3}{4}$ , 64-QAM  $\frac{2}{3}$ , and 64-QAM  $\frac{3}{4}$  for the SM mode.

### 4.1. Channel estimation

We consider pilot-based frequency domain channel estimation for our system [15–17]. At first, the channel response of each pilot subcarrier will be estimated by using a least square (LS) estimator. Then the channel response of the data subcarriers will be estimated by applying linear interpolation and linear extrapolation. We have selected this method because it reduces computational complexity. Moreover, an

LS estimator requires comparatively less amount of prior knowledge. Power level and modulation technique used for the pilot subcarriers are known to the receiver. Our system is a  $2 \times 2$  MIMO OFDMA system and capable of switching between STBC and SM transmission modes. We consider an independent pilot pattern (IPP) approach for MIMO channel estimation [16]. In IPP, two antennas do not transmit the same pilot subcarriers simultaneously.

In case of any pilot subcarrier  $p$  of the  $m$ th OFDMA symbol, the received signal in the frequency domain can be written as

$$Y_{p,m} = H_{p,m} X_{p,m} + W_{p,m} \quad (9)$$

where  $X_{p,m}$  is known to the receiver.  $W_{p,m}$  is the unexpected noise or interference. The objective function of a LS estimator is

$$\min \|Y_{p,m} - \hat{H}_{p,m} X_{p,m}\|^2$$

from which we get the estimated channel response for the pilot subcarrier:

$$\hat{H}_{p,m} = \frac{Y_{p,m}}{X_{p,m}} = H_{p,m} + E_{p,m} \quad (10)$$

where  $E_{p,m} = W_{p,m}/X_{p,m}$  is an error term due to channel noise and imperfection inherent in the LS estimator.

Channel responses for the data subcarriers can be estimated by using linear interpolation or linear extrapolation. The estimated channel response for any data subcarrier  $n$  ( $n$  is the physical index) at the  $m$ th OFDMA symbol is given by

$$\hat{H}_{n,m} = \hat{H}_{p_A,m} + \frac{\hat{H}_{p_B,m} - \hat{H}_{p_A,m}}{p_B - p_A} (n - p_A) \quad (11)$$

where  $p_A$  and  $p_B$  are the pilot subcarrier physical indices and  $p_B > p_A$ . Also  $n$ ,  $p_A$  and  $p_B$  are members of the same cluster. Equation (11) performs linear interpolation where  $p_A < n < p_B$ . It performs linear extrapolation when  $n < p_A$  or  $n > p_B$ .

We can apply the same technique for all the subcarriers and for all the OFDMA symbols. In case of odd OFDMA symbols,  $h_{11}(n)$  and  $h_{12}(n)$  can be estimated. In case of even OFDMA symbols,  $h_{21}(n)$  and  $h_{22}(n)$  can be estimated. Then, the average time can be calculated for the entire downlink subframe.

$$h(n) = \frac{2}{M} \sum_{m=1}^{M-1} \hat{H}_{n,m} \quad \text{for odd symbols,}$$

$$h(n) = h_{11}(n) \text{ or } h_{12}(n) \quad (12)$$

$$h(n) = \frac{2}{M} \sum_{m=2}^M \hat{H}_{n,m} \quad \text{for even symbols,}$$

$$h(n) = h_{21}(n) \text{ or } h_{22}(n) \quad (13)$$

$$\mathbf{H}(n) = \begin{bmatrix} h_{11}(n) & h_{12}(n) \\ h_{21}(n) & h_{22}(n) \end{bmatrix} \quad (14)$$

where  $M$  is the total number of downlink symbols, which is always an even number. Hence, the estimated channel matrix  $\mathbf{H}$  for each subcarrier is sent to the BS *via* uplink. The estimated average channel gain (spatial average) of a subcarrier  $n$  can be defined as

$$\tilde{H}(n) = \sqrt{\frac{1}{4} \sum_{i=1}^2 \sum_{j=1}^2 |h_{ij}(n)|^2} = \frac{1}{2} \|\mathbf{H}(n)\|_{\mathbf{F}} \quad (15)$$

where  $\|\mathbf{H}(n)\|_{\mathbf{F}}$  is the Frobenius norm of the channel matrix.

## 4.2. SNR estimation

Estimated channel gains are used to estimate SNR. In OFDMA, we may separate the weak subchannels from the strong ones, but we do not have that option at the subcarrier level. SNR is highly dependent on power allocation strategy. We leave inter-subchannel power allocation as a component of RA. Here we describe an intra-subchannel power allocation strategy.

Let  $\tilde{H}_k(n)$  be the estimated average channel gain of the  $n$ th subcarrier of the  $k$ th subchannel, and  $s_k(n)$  be the allocated power to that subcarrier. Then the estimated SNR at the receiver end is given by

$$\Gamma_k(n) = \frac{s_k(n) |\tilde{H}_k(n)|^2}{\sigma^2} \quad (16)$$

The estimated effective SNR of the  $k$ th subchannel is given by

$$\Gamma_{k,E} = 2^{\frac{1}{N_k} \sum_{n=1}^{N_k} \log_2(1+\Gamma_k(n))} - 1 \quad (17)$$

where  $N_k$  is the total number of data subcarriers in the  $k$ th subchannel and  $n \in \{1, 2, \dots, N_k\}$ . In our power allocation strategy, we aim for each subcarrier within a subchannel to experience the same SNR. Let  $\Phi_k$  be the allocated power to the  $k$ th subchannel, excluding the power of the pilot subcarriers. According to our power allocation strategy,  $\Phi_k$  is distributed among the member subcarriers in such a way

that

$$\begin{aligned} \frac{s_k(1) |\tilde{H}_k(1)|^2}{\sigma^2} &= \frac{s_k(2) |\tilde{H}_k(2)|^2}{\sigma^2} \\ &= \frac{s_k(3) |\tilde{H}_k(3)|^2}{\sigma^2} = \dots = \Gamma_k(n) \end{aligned} \quad (18)$$

$$\sum_{n=1}^{N_k} s_k(n) = \Phi_k \quad (19)$$

From Equations (18) and (19), we have

$$\Gamma_k(n) = \frac{\Phi_k}{\sum_{n=1}^{N_k} \frac{\sigma^2}{|\tilde{H}_k(n)|^2}} \quad (20)$$

$$\Gamma_{k,E} = 2^{\frac{1}{N_k} N_k \log_2(1+\Gamma_k(n))} - 1 = \Gamma_k(n), \quad \forall n \quad (21)$$

Therefore, the effective SNR of the subchannel is equal to the estimated SNR of an individual data subcarrier.

## 4.3. Threshold tables

We set the SNR thresholds based on the FBER upper bound, which provides better safety margin and lower computational cost. We consider maximal ratio combining (MRC) reception with Alamouti code for the STBC mode [18], and zero forcing (ZF) detection for the SM mode. In threshold, selection does not include SNR gain from a convolutional code (CC) scheme. We select the SNR threshold values for  $q \leq 10^{-3}$ . Two tables are prepared to specify the minimum SNRs per symbol required to maintain  $q \leq 10^{-3}$ . The threshold values for the STBC mode are summarized in Table I. The threshold value selection for the SM mode requires additional information on spatial correlation. We introduce a multiplying factor  $\psi$  as an indicator for spatial correlation (see Appendix I).

$$\psi(n) = \frac{|\Delta(n)|^2}{\|\mathbf{H}(n)\|_{\mathbf{F}}^4} \quad (22)$$

where  $\Delta(n)$  is the determinant of the channel matrix of any subcarrier  $n$ , and  $\|\mathbf{H}(n)\|_{\mathbf{F}}$  is the Frobenius norm of

**Table I.** SNR threshold table for STBC mode ( $q \leq 10^{-3}$ ).

Modulation	CC coding rate	Bit/sym.	Spectral efficiency (bps/Hz)	SNR thres. (dB)
QPSK	$\frac{1}{2}$	2	1	12.5
QPSK	$\frac{3}{4}$	2	1.5	14
16 QAM	$\frac{1}{2}$	4	2	23
16 QAM	$\frac{3}{4}$	4	3	25
64 QAM	$\frac{2}{3}$	6	4	31
64 QAM	$\frac{3}{4}$	6	4.5	32.5

**Table II.** SNR Threshold table for SM mode ( $q \leq 10^{-3}$  and  $\psi \geq 0.1$ ).

Modulation	CC coding rate	Bit/sym.	Spectral efficiency (bps/Hz)	SNR thres. (dB)
16 QAM	$\frac{1}{2}$	4	4	30
16 QAM	$\frac{3}{4}$	4	6	31
64 QAM	$\frac{2}{3}$	6	8	38
64 QAM	$\frac{3}{4}$	6	9	39

the channel matrix. A higher value of  $\psi$  indicates lower spatial correlation and *vice versa*. Higher value of  $\psi$  is more suitable for the SM mode. We set a lower bound for  $\psi$  to select the SNR values for the SM mode. The threshold values for the SM mode are summarized in Table II.

#### 4.4. Throughput maximization

In the previous section, we addressed a throughput maximization problem. In the next subsection, we propose an LA algorithm for that problem. Without using the traditional nonlinear optimization techniques, we can solve it heuristically. The main idea is that ‘if we select the burst profile with the highest spectral efficiency at a given condition, then the throughput will be maximized’. In an ideal case, the channel estimation is perfect; MIMO channels are totally uncorrelated and there is no erroneous reception, etc. In order to adapt with the realistic scenario, we introduce a ‘priority function’ as the constraint in the problem formulation. The NACK message or erroneous reception occurs when the SNR is over estimated. The priority function affects the burst profile selection and works as a protection against successive erroneous reception. With the priority function, the solution automatically contains an adaptive ARQ mechanism.

#### 4.5. Proposed LA algorithm

Before describing our LA algorithm steps, we reiterate some conditions: subchannel allocation and inter-subchannel power allocation are done by the RA algorithm. Our algorithm starts when a subchannel is allocated to a mobile hotspot and the power for that subchannel is also allocated. We assume that frame by frame channel estimation is available. Here, we describe how an appropriate burst profile is selected for a subchannel. Our goal is to perform frame by frame LA for the downlink.

Let  $\gamma_k[u]$  denote the adjusted SNR of the  $k$ th subchannel for the  $u$ th downlink subframe,  $\gamma_k[u-1]$  denote the adjusted SNR of the  $k$ th subchannel for the  $(u-1)$ th downlink subframe,  $\alpha$  denote the adjustment factor,  $\Gamma_{k,E}[u]$  denote the estimated effective SNR of the  $k$ th subchannel for the  $u$ th downlink subframe,  $\Phi_k[u]$  denote the allocated power to the  $k$ th subchannel for the  $u$ th downlink subframe,  $\Phi_k[u-1]$  denote the allocated power to the  $k$ th subchannel for the  $(u-1)$ th downlink subframe,  $\Omega_k[u]$  denote the MIMO threshold function of the  $k$ th subchannel for the  $u$ th

downlink subframe,  $\rho$  denote the ARQ message indicator,  $\psi_{k,GM}[u]$  denote the geometric mean of the estimated multiplying factors of the  $k$ th subchannel for the  $u$ th downlink subframe,  $U_{SM}$  denote the set of the candidate burst profiles for the SM mode,  $U_{STBC}$  denote the set of the candidate profiles for the STBC mode,  $i$  denote the burst profile index,  $p_i$  denote the priority function of the burst profile  $i$ , and  $\eta_i$  denote the spectral efficiency of the burst profile  $i$ .

The AL algorithm is comprised of the following four steps.

##### Step 1. SNR adjustment

An OFDMA frame starts with a downlink subframe and ends with an uplink subframe. A time gap interval takes place between them. The downlink burst profiles are selected based on the feedback information from the previous uplink. We adjust the estimated SNR due to high mobility, and define an adjusted SNR of the  $k$ th subchannel for the  $u$ th downlink subframe as

$$\gamma_k[u] = (1-\alpha)\Gamma_{k,E}[u] + \alpha \frac{\gamma_k[u-1]\Phi_k[u]}{\Phi_k[u-1]}, \quad \alpha \in [0, 1] \quad (23)$$

where adjustment factor  $\alpha = v_{\text{current}}/v_{\text{max}}$ ,  $v_{\text{current}}$  is the current velocity of the mobile hotspot, and  $v_{\text{max}}$  is the maximum velocity of the mobile hotspot (see Appendix II).

We know that SNR depends on the allocated power. The allocated power may not be the same for every downlink subframe. Therefore, we need to extract the channel factor from  $\gamma_k[u-1]$  and then calculate an equivalent SNR for  $\Phi_k[u]$ . That is why  $\gamma_k[u-1]$  is multiplied by the ratio  $\Phi_k[u]/\Phi_k[u-1]$  in the second term of Equation (23).

##### Step 2. MIMO mode selection

We know that the STBC mode performs better in the lower SNR region and the SM mode performs better in the higher SNR region. But SNR information is not enough for the SM mode, it requires an additional information on  $\psi$ . Therefore, we consider both of them in our mode selection procedure. The geometric mean of the estimated multiplying factors ( $\psi$ ) of the  $k$ th subchannel for the  $u$ th downlink subframe is given by

$$\psi_{k,GM}[u] = \left[ \prod_{n=1}^{N_k} \psi_k(n) \right]^{\frac{1}{N_k}} \quad (24)$$

We need to define a function in order to specify SNR information of a particular subchannel for a particular downlink subframe. We call it the MIMO threshold

function. The MIMO threshold function of the  $k$ th subchannel for the  $u$ th downlink subframe is defined as

$$\Omega_k[u] = I_{\{\rho=0\}} I_{\{\gamma_k[u] \geq 30\text{dB}\}} + I_{\{\rho=1\}} I_{\{\gamma_k[u] \geq 31\text{dB}\}} \quad (25)$$

$I_{\{\cdot\}}$  is the indicator function which takes either 1 or 0 depending on satisfaction of condition.  $\rho$  takes the value 0 if the corresponding ARQ block in the previous downlink subframe was successfully received and 1 for erroneous reception.

The MIMO threshold function prevents the formation of feedback loop, i.e., we do not need to change the MIMO mode once we select it for a particular downlink subframe.  $\Omega_k[u]$  specifies two thresholds for the SM mode depending on the ARQ message indicator: 30 dB for  $\rho = 0$  and 31 dB for  $\rho = 1$ .

In a simple manner, if  $\Omega_k[u] = 1$  and  $\psi_{k,\text{GM}}[u] \geq 0.1$ , then select the SM mode. Otherwise select the STBC mode. In the SM mode, the possible burst profile  $i$  is chosen as  $i \in U_{\text{SM}}$ . In the STBC mode, the possible burst profile  $i$  is chosen as  $i \in U_{\text{STBC}}$ .

### Step 3. Priority calculation

The priorities of the burst profile can be calculated by using a modified version of Equations (4) and (5). Here, we use the corresponding SNR threshold instead of FBER. Higher value of the priority function indicates higher spectral efficiency and *vice versa*.

$$p_i(\eta_i, \rho) = \eta_i I_{\{\gamma_k[u] \geq \theta_i\}} \left[ I_{\{i = \arg \max_j \eta_j I_{\{\gamma_k[u] \geq \theta_j\}}\}} I_{\{\rho=0\}} + I_{\{i \neq \arg \max_j \eta_j I_{\{\gamma_k[u] \geq \theta_j\}}\}} I_{\{\rho \geq 0\}} \right] \quad (26)$$

$$\text{for } \sum_i^U I_{\{\gamma_k[u] \geq \theta_i\}} \geq 2$$

$$= \eta_i I_{\{\gamma_k[u] \geq \theta_i\}} \text{ for } \sum_i^U I_{\{\gamma_k[u] \geq \theta_i\}} = 1 \quad (27)$$

where  $\theta_i$  is the SNR threshold of the burst profile  $i$

### Step 4. Burst profile selection

The final step is to select the burst profile with the highest priority.

$$i^* = \arg \max_i p_i(\eta_i, \rho) \quad (28)$$

As the priority function assigns higher priorities to the higher spectral efficiency burst profiles, the burst profile  $i$  will maximize throughput. We repeat the same routine for each subchannel to find the best burst profile.

## 5. NUMERICAL RESULTS

In this section, we present some numerical results on the proposed LA algorithm, which are obtained from downlink

link level simulations using partial Monte Carlo method in MATLAB. In the partial Monte Carlo method, all the processes in a system are not simulated as random processes; some of them are simulated based on statistical models. In this paper, statistical models are used for path loss and noise. We consider some simple scenarios, which are appropriate for evaluating performance of the proposed LA algorithm. We consider a single cell single user (only one mobile hotspot) case. The downlink between a WiMAX BS and the AP of a mobile hotspot is simulated. Two performance metrics are evaluated: FBER and normalized throughput.

We define an ARQ block which consists of one subchannel and two time slots. We choose two non-adjacent physical clusters to construct the subchannel. The simulation parameters are summarized in Table III. The miscellaneous losses include the AP noise figure and any other possible losses. Though the ARQ block is a small part of the whole downlink subframe, we use the term frame to indicate the ARQ block for convenience. Two major categories of investigations are presented: impact of moving direction and impact of velocity-based SNR adjustment.

### 5.1. Impact of moving direction

We consider two cases of moving direction: (1) a mobile hotspot arriving to the cell center (we call it the arriving mobile hotspot), and (2) a mobile hotspot departing from the cell center (we call it the departing mobile hotspot). In both cases the velocity is set to 90 km/h, and the allocated power is set to 0.5 W (27 dBm). The initial distance for the arriving mobile hotspot is 900 m from the BS. The initial distance for the departing mobile hotspot is 150 m from the BS. Numerical results are obtained for 30 s duration (6000 frames).

Figure 3(a) shows the instantaneous FBER plots for the arriving mobile hotspot. It can be seen that the proposed LA algorithm is able to keep the ‘instantaneous FBER’  $\leq 10^{-3}$  most of the time. Figure 3(b) shows the instantaneous normalized throughput plots for the arriving mobile hotspot. It can be seen that the throughput is dominated by the path loss. The throughput increases as the mobile hotspot gets closer to the BS. The path loss decreases with time for the arriving mobile hotspot.

Let us consider the departing mobile hotspot. Figure 4(a) shows the instantaneous FBER plots for the departing mobile hotspot. It reveals that the proposed LA algorithm is able to keep the ‘instantaneous FBER’  $\leq 10^{-3}$  most of the time. Figure 4(b) shows the instantaneous normalized throughput plots for the departing mobile hotspot. It reveals that the throughput is dominated by the path loss. We see that throughput decreases as the mobile hotspot gets further away from the BS. The path loss increases with time for the departing mobile hotspot. Roughly, Figure 4(b) shows a reverse scenario of Figure 3(b) because of opposite moving directions.

**Table III.** Simulation parameters.

Parameter	Description/value
Cell radius	1 km
Allocated power to the subchannel	0.5 W, 1.0 W
BS Antenna gain	16 dBi
BS Antenna height	40 m
Frequency band	2.3 GHz
FFT size	1024
System bandwidth	10 MHz
Symbol duration	115.2 $\mu$ s
Guard ratio	1/8
Thermal noise density	-174 dBm/Hz (at 25°C)
Mobile hotspot velocity	60 km/h, 90 km/h, 120 km/h
Subchannelization strategy	PUSC
Duplex mode	TDD
Channel model	ITU-R Vehicular B
AP antenna height	2.8 m
Shadowing loss	10 dB
Path loss model	COST 231 Hata model for suburban environment (min. separation required 35 m)
Miscellaneous losses	12 dB
AP Antenna gain	10 dB
Fading type	Flat Rayleigh fading
Frame duration	5 ms
DL to UL ratio	3:1
MIMO Antenna configuration	2 $\times$ 2
BS and AP Antenna pattern	Omnidirectional
MIMO mode	STBC, SM (switchable)
Burst size (one ARQ block)	1 subchannel $\times$ 4 symbols
Maximum number of retransmissions	3
$v_{\max}$ settings	360 km/h

## 5.2. Impact of velocity-based SNR adjustment

As the proposed LA algorithm adjusts SNR based on velocity of the mobile hotspots, it is necessary to investigate

the impact of velocity-based SNR adjustment. We separately consider three different cases of velocity: 60, 90, and 120 km/h. These mobile hotspots are the departing mobile hotspots. From the discussion in the previous subsection, we know that the throughput of the departing mobile hotspots

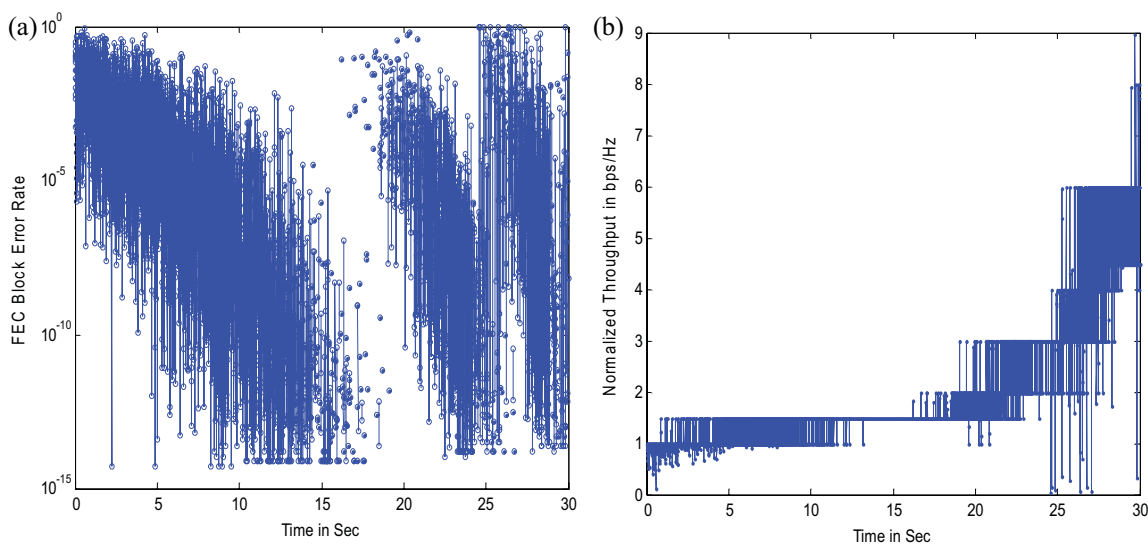


**Figure 3.** (a) Instantaneous FER plots for the arriving mobile hotspot. (b) Instantaneous normalized throughput plots for the arriving mobile hotspot.

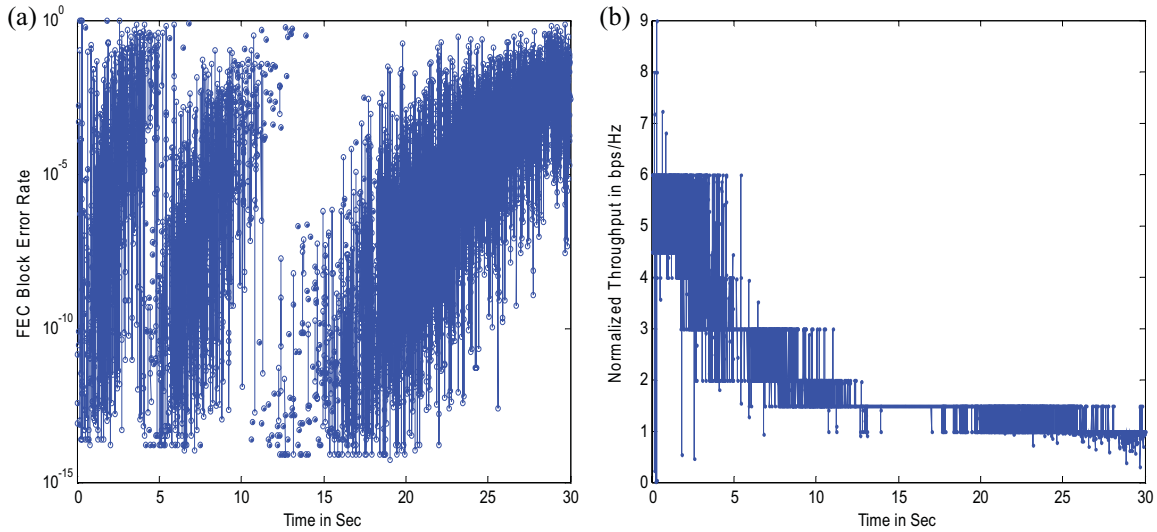


**Figure 4.** (a) Instantaneous FBER plots for the departing mobile hotspot. (b). Instantaneous normalized throughput plots for the departing mobile hotspot.

decreases with time. The initial distance is set at 200 m from the BS. The final location is situated near the cell edge in all cases. The allocated power is set to 1.0 W (30 dBm) in each case. We compare the performance of the SNR adjusted LA with that of the SNR non-adjusted LA (just omitting the first step of the proposed LA algorithm). We compare the average performance within a 2-second interval.

Firstly, we consider a mobile hotspot with velocity 60 km/h. Numerical results are obtained for 25 s duration (5000 frames). Figure 5(a) and (b) shows the comparative throughput and FBER performance, respectively. We see that velocity-based SNR adjustment performs better than the non-adjusted SNR in both perspectives.

The velocity-based SNR adjustment improves throughput and reduces FBER. Overall average of the normalized throughput is 2.2154 bps/Hz for the velocity-based SNR adjustment, whereas that for the non-adjusted SNR is 2.2045 bps/Hz. Overall average of the FBER is 0.0107 for the velocity-based SNR adjustment, whereas that for the non-adjusted SNR is 0.0110. Secondly, we consider a mobile hotspot with velocity 90 km/h. Numerical results are obtained for 22 s duration (4400 frames). Figure 6(a) and (b) shows the comparative throughput and FBER performance, respectively. We see that velocity-based SNR adjustment performs better than the non-adjusted SNR in both perspectives.

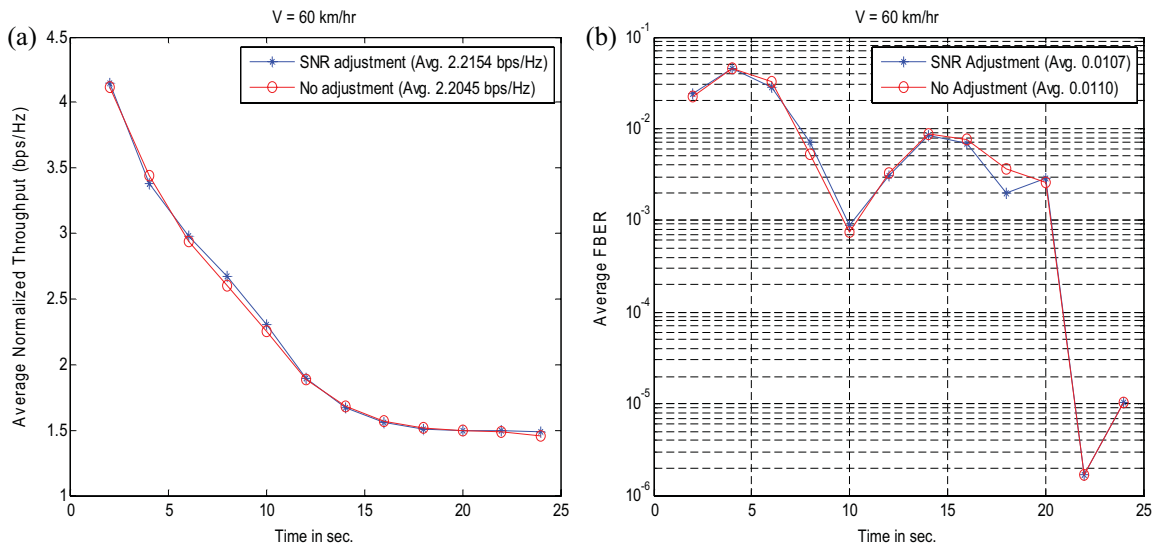


**Figure 5.** (a) Impact of SNR adjustment on the throughput with velocity 60 km/h. (b) Impact of SNR adjustment on the FBER with velocity 60 km/h.

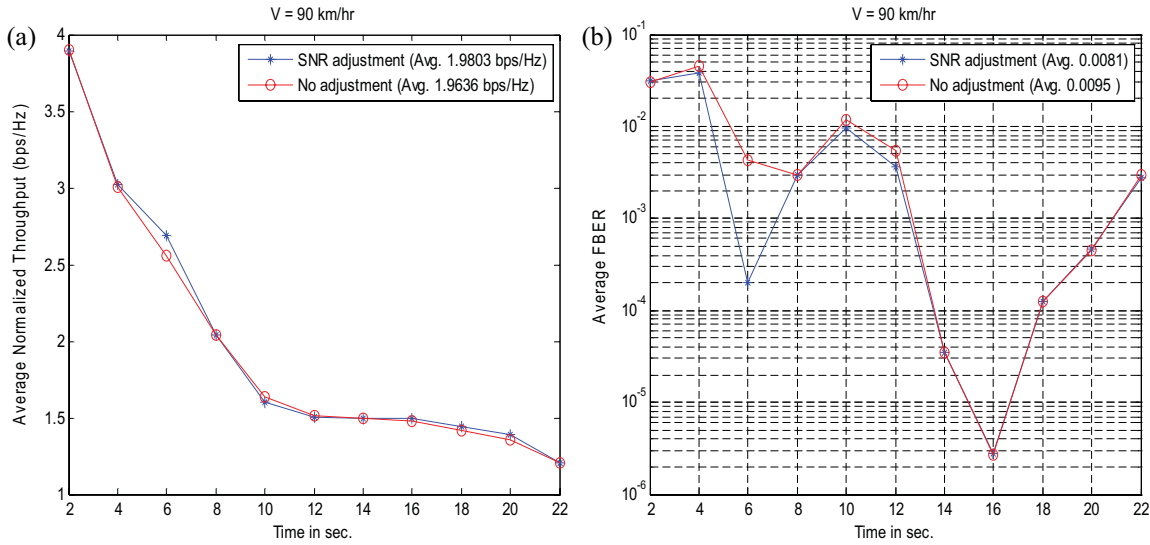


**Figure 6.** (a) Impact of SNR adjustment on the throughput with velocity 90 km/h. (b) Impact of SNR adjustment on the FBER with velocity 90 km/h.

The velocity-based SNR adjustment improves throughput and reduces FBER. Overall average of the normalized throughput is 1.9803 bps/Hz for the velocity-based SNR adjustment, whereas that for the non-adjusted SNR is 1.9636 bps/Hz. Overall average of the FBER is 0.0081 for the velocity-based SNR adjustment, whereas that for the non-adjusted SNR is 0.0095. Finally, we consider a mobile hotspot with velocity 120 km/h. Numerical results are obtained for 20 s duration (4000 frames). Figure 7(a) and (b) shows the comparative throughput and FBER performance, respectively. We see that velocity-based SNR adjustment performs better than the non-adjusted SNR in both of the perspectives. The velocity-based SNR adjust-

ment improves throughput and reduces FBER. Overall average of the normalized throughput is 1.8225 bps/Hz for the velocity-based SNR adjustment, and the FBER is 0.0080 for the velocity-based SNR adjustment, whereas that for the non-adjusted SNR is 0.0100.

Now we discuss a common feature among the Figures 5(b), 6(b), and 7(b). In some intervals FBER exhibits very low values. This happens due to better accuracy in channel estimation and/or reduced number of over estimation of SNR.

According to the discussions above, we can conclude that the velocity-based SNR adjustment improves overall performance. This improvement comes in the form of

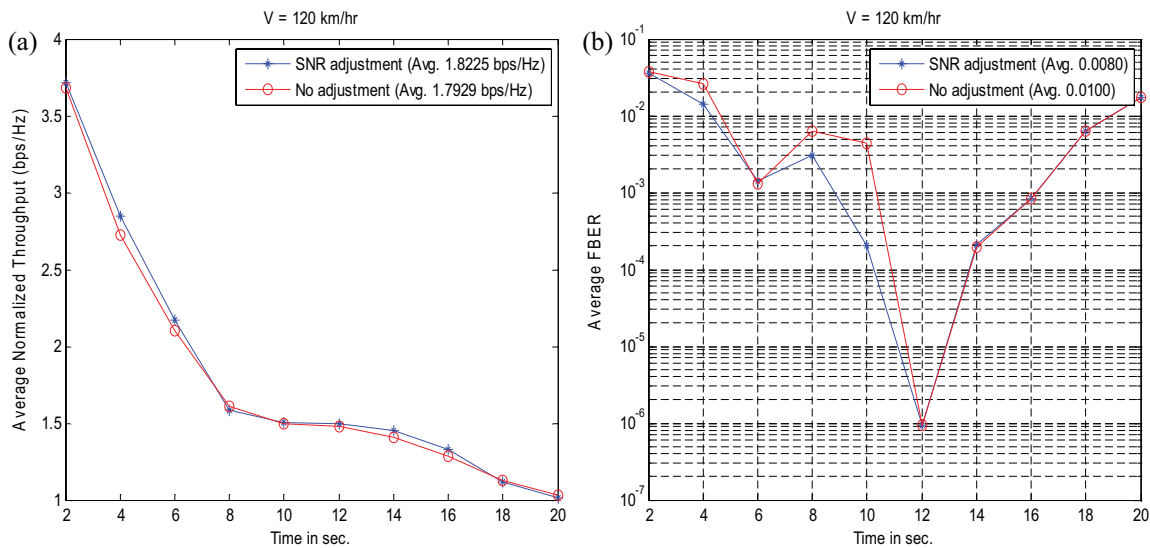


**Figure 7.** (a) Impact of the SNR adjustment on the throughput with velocity 120 km/h. (b) Impact of SNR adjustment on the FBER with velocity 120 km/h.

both increased throughput and reduced FBER. Velocity-based SNR adjustment becomes more effective at higher velocities.

## 6. CONCLUSIONS

In this paper, we have proposed a simple LA algorithm for the WiMAX supported mobile hotspots. The algorithm has been designed for the downlink part between the WiMAX BS and mobile hotspot AP. It is an instantaneous SNR-based LA algorithm. The link level performance of the proposed algorithm has also been evaluated. Path loss has a dominant effect on throughput, and moving direction is a key factor that influences the behavior of throughput *versus* time characteristics. In most of the cases, the proposed LA algorithm is able to keep FBER under a certain value. The proposed LA algorithm, capable of working under various types of conditions, is independent of RA. It is adaptive with velocity, power, direction, channel response, and system performance. Though the proposed LA algorithm is for the mobile WiMAX network, it can be extended to any other MIMO-OFDMA networks.

## ACKNOWLEDGEMENTS

This work has been supported by the Natural Sciences and Engineering Research Council (NSERC) of Canada under grant no. RGPIN7779.

## 7. APPENDIX I

### 7.1. Derivation of multiplying factor $\psi$

The multiplying factor relates estimated SNR with post-detection SNR for SM mode. ZF detection requires computing pseudo inverse of MIMO channel matrix. In case of a  $2 \times 2$  MIMO configuration, pseudo inverse and inverse are the same. The inverse of channel matrix is given by

$$\begin{aligned} \mathbf{G}(n) &= \mathbf{H}(n)^{-1} \\ &= \begin{bmatrix} \frac{h_{22}(n)}{h_{11}(n)h_{22}(n) - h_{12}(n)h_{21}(n)} & \frac{-h_{12}(n)}{h_{11}(n)h_{22}(n) - h_{12}(n)h_{21}(n)} \\ \frac{-h_{21}(n)}{h_{11}(n)h_{22}(n) - h_{12}(n)h_{21}(n)} & \frac{h_{11}(n)}{h_{11}(n)h_{22}(n) - h_{12}(n)h_{21}(n)} \end{bmatrix} \\ &= \frac{1}{\Delta} \begin{bmatrix} h_{22}(n) & -h_{12}(n) \\ -h_{21}(n) & h_{11}(n) \end{bmatrix} \end{aligned} \quad (29)$$

where  $\Delta = \det(\mathbf{H}(n)) = h_{11}(n)h_{22}(n) - h_{12}(n)h_{21}(n)$ . For convenience, in what follows we drop the subcarrier index.

$$\begin{aligned} [\mathbf{G}\mathbf{G}^H] &= \frac{1}{|\Delta|^2} \begin{bmatrix} |h_{22}|^2 + |h_{12}|^2 & -h_{11}^*h_{12} - h_{21}^*h_{22} \\ -h_{11}h_{12}^* - h_{21}h_{22}^* & |h_{11}|^2 + |h_{21}|^2 \end{bmatrix} \end{aligned} \quad (30)$$

In the SM mode two symbols are transmitted simultaneously using two different antennas. Allocated power to a subcarrier is divided by two, SNR for the first symbol and second symbol can be written as

$$\Gamma_1 = \frac{s|\Delta|^2}{2\sigma^2(|h_{22}|^2 + |h_{12}|^2)} \quad \text{and} \quad \Gamma_2 = \frac{s|\Delta|^2}{2\sigma^2(|h_{11}|^2 + |h_{21}|^2)}$$

We need to consider both antennas (i.e., all the spatial channels) in order to set a threshold value. Taking a simple average of the denominators, we obtain an interesting expression for post-detection SNR for the SM mode with ZF detection

$$\Gamma_{SM} = \frac{s|\Delta|^2}{\sigma^2(|h_{22}|^2 + |h_{12}|^2 + |h_{11}|^2 + |h_{21}|^2)} = \frac{s|\Delta|^2}{\sigma^2 \|\mathbf{H}\|_F^2} \quad (31)$$

The estimated SNR is expressed as

$$\Gamma = s |\tilde{H}|^2 / \sigma^2 = s \|\mathbf{H}\|_F^2 / 4\sigma^2 \quad (32)$$

The post-detection SNR for the SM mode with ZF detection can be written as

$$\Gamma_{SM} = \frac{s|\Delta|^2}{\sigma^2 \|\mathbf{H}\|_F^2} = \frac{s \|\mathbf{H}\|_F^2}{4\sigma^2} \frac{4|\Delta|^2}{\|\mathbf{H}\|_F^4} = 4\psi\Gamma \quad (33)$$

where  $\psi = |\Delta|^2 / \|\mathbf{H}\|_F^4$  is the multiplying factor.

## 8. APPENDIX II

### 8.1. Selection of adjustment factor $\alpha$

We introduce the parameter  $\alpha$  to include the impact of mobility in SNR estimation. We define  $\alpha$  as the ratio of current Doppler shift to maximum tolerable Doppler shift:

$$\alpha = \frac{f_{D,current}}{f_{D,max}} = \frac{v_{current}}{v_{max}} \quad (34)$$

where  $v_{current}$  and  $v_{max}$  are the current velocity and the maximum velocity of a mobile hotspot, respectively. The BS can get the exact value of the current velocity from mobile hotspot.

The upper bound of  $v_{max}$  can be obtained as follows:

maximum Doppler shift < subcarrier spacing, (This condition avoids the impact of Doppler's effect.)

$$\begin{aligned} \text{or, } \frac{v_{max}f_c}{c} &< \Delta f \\ \text{or, } v_{max} &< \frac{c\Delta f}{f_c} \end{aligned} \quad (35)$$

This upper bound is very loose because signal power does not confine within the center frequency. We define a spreading margin, which is the difference between subcarrier spacing and subcarrier bandwidth ( $BW_{SC}$ ). It will help

us to ignore intercarrier interference (ICI). Spreading margin is the maximum tolerable frequency spreading without any overlapping between two successive subcarriers. In our system  $\Delta f = 10.94$  kHz and  $BW_{SC} = 9.76$  kHz.

We use spreading margin to find the upper bound of  $v_{\max}$  as follows:

$$v_{\max} < \frac{c}{f_c} (\Delta f - BW_{SC}) \quad (36)$$

$$\text{or, } v_{\max} < 554 \text{ km/h} \quad (37)$$

We choose 360 km/h as  $v_{\max}$ , and leave some portion for frequency offset effect. Frequency spread occurs due to Doppler spread and subcarrier (carrier) frequency offset effect [19]. In reality, the mobile hotspot will never be operated with velocity  $v_{\max}$ . We define  $v_{\max}$  as the velocity, at which channel estimation does not work at all. In other words, the channel is totally untraceable at  $v_{\max}$ .

## REFERENCES

1. Ho D, Valaee S. Information raining and optimal link-layer design for mobile hotspots. *IEEE Transactions on Mobile Computing* 2005; **4**(3): 271–284.
2. Chung AYT, Hassan M. Traffic distribution schemes for multi-homed mobile hotspots. *Proceedings of VTC Spring 2005*, Stockholm, Sweden, May 2005; 2127–2131.
3. Iera A, Molinaro A, Polito S, Ruggeri G, Vilasi A. Gateway discovery and selection in mobile hotspot. *Proceedings of Auswireless 2006*, Sydney, Australia, March 2006.
4. Pack S, Rutagemwa H, Shen X, Mark JW, Cai L. An integrated WWAN-WLAN link model in mobile hotspots. *Proceedings of Chinacom 2006*, Beijing, China, October 2006.
5. Pack S, Rutagemwa H, Shen X, Mark JW, Cai L. Performance analysis of mobile hotspots with heterogeneous wireless links. *IEEE Transactions on Wireless Communications* 2007; **6**(10): 3717–3727.
6. Pack S, Shen X, Mark JW, Cai L. Throughput analysis of TCP-friendly rate control in mobile hotspots. *IEEE Transactions on Wireless Communications* 2008; **7**(1): 193–203.
7. Mobile WiMAX part I: a technical overview and performance evaluation. *WiMAX Forum*, August 2006.
8. Marquet B, Biglieri E, Sari H. MIMO link adaptation in mobile WiMAX systems. *Proceedings of IEEE WCNC 2007*, Hong Kong, March 2007; 1810–1813.
9. Marabissi D, Tarchi D, Genovese F, Fantacci R. Adaptive modulation in wireless OFDMA systems with finite state modeling. *Proceedings of IEEE Globecom 2007*, Washington, DC, USA, November 2007; 5210–5214.
10. Chan TH, Hamdi M, Cheung MM. A link adaptation algorithm in MIMO-based WiMAX systems. *Journal of Communications* 2007; **2**(5): 16–24.
11. Demmel JW. The probability that a numerical analysis problem is difficult. *Mathematics of Computation* 1998; **50**(182): 449–480.
12. Heath RW, Paulraj AJ. Switching between diversity and multiplexing in MIMO systems. *IEEE Transactions on Communications* 2005; **53**(6): 962–968.
13. Nuaymi L. *WiMAX Technology for Broadband Wireless Access*. John Wiley and Sons Ltd: Hoboken, NJ, USA, 2007.
14. Andrews JG, Ghosh A, Muhamed R. *Fundamentals of WiMAX*. Prentice Hall publishers: Upper Saddle River, NJ, USA, 2007.
15. Raghavendra MR, Lior E, Bhashyam S, Giridhari K. Parametric channel estimation for pseudo-random tile-allocation in uplink OFDMA. *IEEE Transactions on Signal Processing* 2007; **55**(11): 5370–5381.
16. Kim T, Andrews JG. Optimal pilot-to-data power ratio for MIMO-OFDM. *Proceedings of IEEE Globecom 2005*, St. Louis, MO, December 2005; 1481–1485.
17. Cai J, Shen X, Mark JW. EM channel estimation algorithm for OFDM wireless communication systems. *Proceedings of IEEE PIMRC 2003*, Beijing, China, September 2003; 804–808.
18. Alamouti SM. A simple transmit diversity technique for wireless communications. *IEEE Transactions on Selected Areas in Communications* 1998; **16**(8): 1451–1458.
19. Lee J, Lou H, Toumpakaris D, Cioffi JM. Effect of carrier frequency offset on OFDM systems for multipath fading channels. *Proceedings of IEEE Globecom 2004*, Dallas, TX, November 2004; 3721–3725.

## AUTHORS' BIOGRAPHIES



**Md. M. Hasan** was born in Jamalpur, Bangladesh in 1979. He received B.Sc. and M.Sc. in Electrical and Electronic Engineering from Bangladesh University of Engineering and Technology (BUET), Dhaka, in 2003 and 2005 respectively. He received M.A.Sc. in Electrical and Computer Engineering from the University of Waterloo, ON, Canada, in 2009. In 2004–06, he worked for several Telecom companies in Bangladesh as an operation and maintenance engineer. He is experienced on multi-vendor telecom equipments. In 2007–09, he worked at center for wireless communications (CWC), Waterloo as a research assistant. His research interests include mobility management, resource allocation, and broadband power line communications. He is a student member of IEEE.



**Jon W. Mark** is a Distinguished Professor Emeritus and the Director of the Centre for Wireless Communications, Department of Electrical and Computer Engineering, University of Waterloo. Upon receiving the Ph.D. degree in electrical engineering from McMaster University, he joined the Department of Electrical Engineering (renamed the Department of Electrical and Computer Engineering in 1989), University of Waterloo, Canada, in 1970. He served as the department Chairman from 1984 to 1990. With a \$1 million donation from Ericsson Canada as seed money, he established the Centre for Wireless Communications at the University of Waterloo in 1996, and has since been serving as the founding Director. His current research interests are in wireless communications and networking, with a focus on resource management, mobility management, cross-layer design, and end-to-end information delivery with QoS provisioning. A Fellow of the IEEE and a Fellow of the Canadian Academy of Engineering, he is the recipient of the *2000 Canadian Award in Telecommunications Research*. He co-authored the text, *Wireless Communications and Networking*, published by Prentice-Hall in 2003. He was the Editor for *Wide Area Networks of the IEEE Transactions on Communications* from 1983 to 1989, the Technical Program Chairman of Infocom'89, a member of the Inter-Society Steering Committee of the IEEE/ACM Transactions on Networking from 1992 to 2003, an Editor of the ACM journal of *Wireless Networks* from 1993 to 2004, and an Associate Editor of the journal of *Telecommunication Systems* from 1994 to 2004.



**Xuemin (Sherman) Shen** received the B.Sc.(1982) degree from Dalian Maritime University (China) and the M.Sc. (1987) and Ph.D. degrees (1990) from Rutgers University, New Jersey (USA), all in electrical engineering. He is a Professor and University Research Chair, Department of Electrical and Computer Engineering, University of

Waterloo, Canada. Dr. Shen's research focuses on resource management in interconnected wireless/wired networks, UWB wireless communications networks, wireless network security, wireless body area networks and vehicular ad hoc and sensor networks. He is a co-author of three books, and has published more than 400 papers and book chapters in wireless communications and networks, control and filtering. Dr. Shen served as the Technical Program Committee Chair for IEEE VTC'10, the Symposia Chair for IEEE ICC'10, the Tutorial Chair for IEEE ICC'08, the Technical Program Committee Chair for IEEE Globecom'07, the General Co-Chair for Chinacom'07 and QShine'06, the Founding Chair for IEEE Communications Society Technical Committee on P2P Communications and Networking. He also served as a Founding Area Editor for IEEE Transactions on Wireless Communications; Editor-in-Chief for Peer-to-Peer Networking and Application; Associate Editor for IEEE Transactions on Vehicular Technology; Computer Networks; and ACM/Wireless Networks, etc., and the Guest Editor for IEEE JSAC, IEEE Wireless Communications, IEEE Communications Magazine, and ACM Mobile Networks and Applications, etc. Dr. Shen received the Excellent Graduate Supervision Award in 2006, and the Outstanding Performance Award in 2004 and 2008 from the University of Waterloo, the Premier's Research Excellence Award (PREA) in 2003 from the Province of Ontario, Canada, and the Distinguished Performance Award in 2002 and 2007 from the Faculty of Engineering, University of Waterloo. Dr. Shen is a registered Professional Engineer of Ontario, Canada, an IEEE Fellow, and a Distinguished Lecturer of IEEE Communications Society.